ACS APPLIED POLYMER MATERIALS

pubs.acs.org/acsapm Article

# Monovalent and Divalent Ions Impair Recovery of Strength when Self-Healing Is Facilitated by Hydrogen Bonding

Durnian C. Parulski-Seager, Amanda Suarez, and Bezawit A. Getachew*

Cite This: ACS Appl. Polym. Mater. 2023, 5, 6143−6150 Read Online

ACCESS | Metrics & More | Article Recommendations | Supporting Information

**ABSTRACT:** Self-healing materials are those that can recover from physical or chemical damage autonomously. To be applied in underwater applications such as water treatment, self-healing materials need to demonstrate sufficient healing ability in complex water matrices. Herein, we investigated how monovalent (NaCl) and divalent ($MgSO_4$) ions at concentrations relevant to brackish and seawater salinity impact the self-healing efficiency of a model 2-acrylamido-2-methyl-1-propanesulfonic acid (AMPS) and *N*,*N*′-methylenebis(acrylamide) (MBA) hydrogel. It has been assumed that divalent ions would form ionic bonds and act as crosslinkers between viable functional groups (negatively charged oxygens, etc.). However, our results suggest that this assumption needs to be reconsidered. Under concentrations relevant to seawater (35 g/L), magnesium ions hindered self-healing efficiency by ∼30% as measured by recovery of ultimate tensile (UT) strength. On the other hand, they improved self-healing efficiency by ∼100% as measured by recovery of UT strain. A similar trend was also observed for sodium ions. The chemical crosslinker ratio when doubled did not impact self-healing efficiency. These results challenge the assumption that divalent ions always form ionic bonds that enhance healing and that chemical crosslinking alters the self-healing performance.

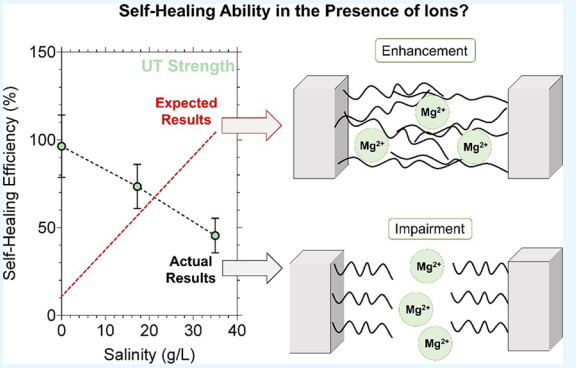


**KEYWORDS:** *smart material, polymer, self-healing, hydrogen bonding, ions*



## 1. INTRODUCTION

Over time, materials degrade from physical and chemical wear, which results in mechanical failure. This compromises safety and reduces the lifetime of systems that rely on these materials for critical functions. For example, the formation of microcracks in airplane fuselage or wings can result in catastrophic accidents, cracks in concrete used for housing and bridges can lead to structure collapse, or a small scratch in protective coatings on metal surfaces can cause severe corrosion. In addition to safety concerns, the need to replace damaged materials creates waste and leads to system downtime, which results in process inefficiencies. To combat this issue, materials that can recover from physical and chemical wear autonomously (self-healing materials) have been explored and developed in the past few decades.[1] Inspired by the phenomena seen in the human body as well as plants, these materials can recover from damage with the help of external stimuli (high temperature, pH, and UV light) or without the need for any intervention at all.[2,3] Self-healing materials have been studied for applications in the aerospace industry, water purification, soft electronics, corrosion protective coatings, and biomedical applications.[4−7]

These materials can heal via two different mechanisms, which are defined as extrinsic or intrinsic. Extrinsic self-healing materials incorporate an embedded, encapsulated healing agent that is released upon damage. The released healing agent covers the damaged area and reacts with the outside environment to solidify in place. In contrast, intrinsic self-healing materials rely on the underlying physical and chemical bonds that hold materials together. These bonds include covalent, supramolecular, and ionic as well as polymer chain entanglements. If these bonds are broken, they can reform. This results in self-healing and restoration of the material's original properties.[1] Due to their reliance on a material's physical and chemical interactions to grant healing instead of a healing agent, intrinsic self-healing materials can recover from repeated damage. This is desired for long-term mechanical integrity and chemical resistance. Of the different intrinsic self-healing mechanisms, supramolecular chemistry is advantageous because of the fast reversibility (dynamic dissociation/association) of the bonds under ambient conditions. Due to the rapid reversibility, an equilibrium state is quickly reached. Supramolecular chemistry includes hydrogen bonding, metal−

Received: April 17, 2023
Accepted: June 26, 2023
Published: July 13, 2023

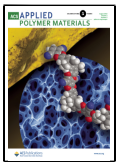

ligand coordination, guest−host interactions, $\pi-\pi$ stacking, ionic bonding, and hydrophobic interactions.[8]

Current developments in intrinsic self-healing have focused on material design, examining self-healing ability of common polymers, and improving mechanical robustness. For example, some studies have provided new, controlled-architecture macromolecules with specific placement of functional groups,[9] and others have studied the self-healing properties of commodity polymers such as poly(methyl methacrylate)/*n*-butyl acrylate [*p*(MMA/*n*BA)] and their derivatives.[10] In addition, much effort has been made to ensure that these materials are strong but also have self-healing properties.[5,7,11−16] Physical and chemical bonds that can reform easily are inherently weaker and result in low mechanical strength; therefore, there needs to be a balance between mechanical robustness (strength and toughness) and dynamic healing. If the material is too rigid, it will prevent flexibility and reformation of noncovalent bonds. Thus far, this balance has been achieved by having a "hard phase" that imparts rigidity, while a "soft phase" allows for toughness and healing. It was found that these materials are mechanically tough due to the breaking of the weaker covalent bonds that dissipate energy.[11] This type of design has been implemented in self-healing materials through multivalent and multi-strength hydrogen bonding, metal−ligand bonds, ionic bonds, and guest−host interactions.[5,7,12−16]

Although progress has been made in the design of self-healing polymers in the past two decades, most self-healing polymers are designed to operate in inert, single-component systems.[1,9,17−21] This presents a challenge in translating these materials into real-world applications where the environment is complex (presence of moisture, ions, natural organic matter, varying pH, high/low temperature, etc.). To be successfully integrated into real-world applications, self-healing polymers need to retain their functionality within these environments; therefore, it is crucial to gain an understanding of how these factors influence self-healing chemistries. Gaining a fundamental understanding will allow us to design polymers such that the natural environment has a neutral impact on healing or enhances it.

Some work has been done to evaluate the use of self-healing materials for corrosion protection coatings in the presence of sodium chloride (monovalent ion).[6] However, these studies focused on extrinsic self-healing materials.[22] Other work has been done to study the healing ability of intrinsic materials in the presence of monovalent and divalent ions; these materials relied on metal−catechol chemistry or ionic bonding to heal.[16,23−26] The studies that focused on metal−catechol chemistry found that divalent ions, $Ca^{2+}$ or $Mg^{2+}$, enhance self-healing, but there is a concentration upper limit to which $Ca^{2+}$ or $Mg^{2+}$ improve healing efficiency. After reaching that limit, the polymer chains can become too rigid, i.e., fewer metal−ligand bonds can reform, and self-healing ability is impaired.[23,24] Materials that employed ionic bonding found that monovalent ions, $Na^{+}$ and $Cl^{-}$, disrupted ionic bonding. This resulted in a lower ultimate tensile (UT) strength[16,26] and higher UT strain.[25,26] With this insight, we know that healing facilitated by metal−ligand bonds may be effective at lower salinity concentrations but lose functionality at higher concentrations.

To improve our understanding of how commonly occurring ions impact intrinsic self-healing of a polymer that heals via hydrogen bonding and interchain diffusion, we investigated how the presence of monovalent (NaCl) and divalent ($MgSO_4$) ions influence the self-healing ability of a model polymer, poly(2-acrylamido-2-methyl-1-propane sulfonic acid) (PAMPS) crosslinked with *N*,*N*′-methylenebis(acrylamide) (MBA) (Figure 1). PAMPS was chosen since its self-healing ability has been previously demonstrated[4,27−29] and due to its ease of synthesis. In addition, this polymer has found use in a variety of applications such as self-healing membranes for water filtration,[4,27,28] proton exchange membranes in fuel cells,[30] and superabsorbents for decontaminating water.[31,32] We hypothesized that monovalent ions would disrupt hydrogen bonding by shielding the interactions between the hydrogen accepting and donating groups. This would hinder self-healing ability via chemical interactions but enhance self-healing via interchain diffusion.[25,26] In contrast, we hypothesized that the positively charged divalent ions would form ionic or metal−ligand interactions with the partially and fully negatively charged oxygen groups.[23,24,27,33] This would improve self-healing via chemical interactions but disrupt self-healing via interchain diffusion. The results of this study can help guide the selection and design of self-healing materials for applications in complex water matrices and bring us closer to creating more resilient and sustainable polymers.

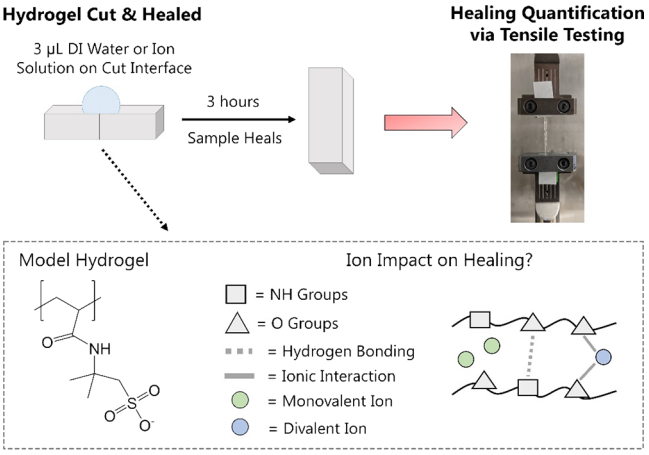


**Figure 1.** Materials and methods. Poly(2-acrylamido-1-propane sulfonic acid) crosslinked with *N*,*N*′-methylenebis(acrylamide) served as a model hydrogel. Samples were cut in half and then healed in the absence of ions (DI water) or in the presence of monovalent (NaCl) or divalent ($MgSO_4$) ions. To quantify the impact of these ions on healing ability, bulk mechanical properties were obtained via tensile testing.

## 2. MATERIALS AND METHODS

**2.1. Materials.** 2-Acrylamido-2-methyl-1-propanesulfonic acid (AMPS, 99%), *N*,*N*′-methylenebis(acrylamide) (MBA, 99%), and sodium chloride (NaCl) were obtained from Sigma-Aldrich. Magnesium sulfide ($MgSO_4$, ≥99%) was purchased from J.T. Baker. Deionized (DI) water was obtained from a Millipore Milli-Q lab water system (conductivity 18.2 MΩ cm at 25 °C).

**2.2. Hydrogel Synthesis and Characterization.** Hydrogels were synthesized via a heat-initiated cationic polymerization process.[28,29] This synthesis process was chosen instead of free radical polymerization due to ease of synthesis. Compared to the commonly used free radical polymerization, heat-initiated cationic polymerization does not require additional chemical reagents (initiator or accelerator) to start the polymerization process; it only requires high temperatures. Aqueous solutions containing 40 wt % monomer (AMPS) and 0.0897 or 0.1764 wt % crosslinker (MBA) were


https://doi.org/10.1021/acsapm.3c00805
ACS Appl. Polym. Mater. 2023, 5, 6143−6150

prepared using DI water. To remove air bubbles, these solutions were degassed for 1 min using a sonicator bath. Reaction solution (5 mL) was pipetted into hexagonal weigh boats, covered in aluminum foil, and placed in an oven at 80 °C for 3 h. Hydrogels were stored in a Memmert HCP 50 humidity chamber at 40 °C and 55% relative humidity (RH).

A Thermo Fisher Scientific Nicolet iS50 FTIR spectrometer was used for FTIR analysis. Pure AMPS and MBA powder were characterized as is. PAMPS/MBA hydrogels were dried overnight under a snorkel to remove water prior to FTIR analysis. Thirty-two scans of each sample were collected.

A Bruker AV III HD 500 MHz spectrometer was used for $^1$H NMR analysis. The NMR spectra were obtained for pure AMPS, pure MBA, and PAMPS hydrogel. The solvent deuterium oxide ($D_2O$) with trimethylsilylpropanoic acid (TSP) was used to prepare samples. PAMPS/MBA hydrogels were synthesized, as described above, but used $D_2O$ as the solvent. Following synthesis, the hydrogels were cut into strips, placed in the NMR tube, and swollen in $D_2O$. The water suppression mode was used for all samples to remove the water peak from the spectrum (AMPS is hygroscopic).

**2.3. Self-Healing Tests.** Tensile testing was selected to assess self-healing.[5,7,12,13,15,16,23−26,34] Samples for testing were prepared by cutting the hydrogels into strips (30−40 mm × 0.75−1.4 mm × 0.8−1.1 mm; length × width × thickness). To obtain a material that was suitable for tensile testing, samples were equilibrated in a Memmert HCP 50 humidity chamber at 40 °C, 45% RH for at least 3 h. They were then cut in half using a guillotine cutter, and the cut interfaces immediately realigned. DI water or salt (NaCl or $MgSO_4$) solution (3 μL) was pipetted onto the cut interface (see Table 1 for salt concentrations used). Samples were left to heal at 40 °C, 45% RH for 3 h. Using an ARES G2 rheometer, tensile stress−strain curves were obtained. Samples were pulled at room temperature and at a rate of 0.1 mm/s. The normal/axial force of the instrument ranged from 0.001 to 20 N. From these stress−strain curves, the UT strength and strain[25,35] were extracted and used to quantify self-healing. Uncut samples and samples healed with DI water served as controls. Self-healing efficiency was calculated using eq 1. All conditions were tested in at least triplicate (see Tables S1 and S2 for the number of parallel samples tested for each condition).

**Table 1. Concentration of Salt Solutions for Self-Healing Tests**[a]

| | Salinity (g/L) | Concentration NaCl (M) | Concentration $MgSO_4$ (M) |
|---|---|---|---|
| Brackish Water | 17.3 | 0.295 | 0.143 |
| Seawater | 35.0 | 0.599 | 0.291 |

[a]These concentrations were calculated based on the typical salinities observed in brackish and seawater.

$$\text{SE}\ (\%) = \frac{\text{MP}_{\text{Cut Sample}}}{\text{MP}_{\text{Pristine Sample}}} \times 100 \quad (1)$$

where SE is the self-healing efficiency and MP is the mechanical property (UT strength or UT strain).

## 3. RESULTS AND DISCUSSION

**3.1. Hydrogel Characterization and Optimization.** The conversion of AMPS to PAMPS is achieved through a heat-initiated cationic polymerization process. Although FTIR spectroscopy is often employed to monitor the polymerization process, the C=C bond that disappears during polymerization is overshadowed by other peaks in the spectra (Figure S1). Therefore, we monitored and confirmed the conversion via $^1$H NMR spectroscopy. Three multiplet peaks were expected from the three hydrogens on the C=C double bond at 6.48, 6.09, and 5.74 ppm on the AMPS spectrum. With the addition of a hydrogen to the terminal carbon and the formation of a new C−C bond connecting two monomers during polymerization (i.e., the presence of two new hydrogen environments), we anticipated the formation of two new peaks in the range of 1.5−2.5 ppm and the shrinkage or disappearance of the multiplets that correspond to the hydrogens surrounding the C=C. As expected, in the AMPS spectra, we see multiplet peaks from 6.13 to 6.31 ppm, a singlet peak at 1.54 ppm, and a singlet peak at 3.43 ppm, which correspond to the three hydrogens surrounding the C=C double, the six hydrogens on the two methyl groups, and the two hydrogens on the carbon neighboring the sulfur atom, respectively (Figure 2a). In the PAMPS spectra, a broad new peak is present at 1.95 ppm, which represents the new hydrogen environments at the point of polymerization (Figure 2b) along with the other peaks present in the AMPS spectra. The presence of a broad singlet at 1.95 ppm rather than the expected multiplet is likely due to variations in the chain lengths and network formation, which result in variable positioning of the relevant atoms. The peaks from 6.13 to 6.31 ppm are still present in the PAMPS spectrum but have decreased by about a factor of 10, which indicates that some unreacted ends remain but at a relatively low concentration.

Following confirmation of the polymerization process, the polymer sample properties were optimized so that the sample's mechanical properties fell below the instrument's maximum normal/axial force (20 N). Four factors influence the mechanical properties of a hydrogel: the monomers used, crosslinking density, polymerization conditions, and degree of swelling.[36] The monomers and the polymerization conditions were kept consistent, while crosslinking density (MBA to AMPS ratio) and degree of swelling (i.e., water content) were varied to optimize the mechanical properties. Large amounts of crosslinker result in stronger, more rigid materials. However, too much crosslinker could result in a material too rigid to self-heal because the chains need to be mobile enough to diffuse across the cut interface and for the non-covalent interactions to be reformed.[35] Too low of a crosslinker ratio could result in polymer samples that are mechanically weak or completely untangle in water. At a given crosslinker ratio, a higher water content results in a softer material, while less water content gives a tougher material.[29,36]

We relied on previous work in the literature that used a 0.001 MBA:AMPS ratio[27] as the starting point for our optimization and tested the crosslinker ratio and humidity levels given in Table S3. We found that crosslinker ratios of 0.003 and 0.006 MBA:AMPS and a relative humidity and temperature of 45% and 40 °C, respectively, resulted in samples that were suitable for testing (Figure S2). At the other MBA:AMPS ratios tested, $1 \times 10^{-4}$ and 0.009, the gel became a viscous liquid when swollen in DI water or exceeded the axial force range of the rheometer, respectively.

**3.2. Self-Healing of PAMPS Polymers in the Absence of Ions.** The self-healing property of the PAMPS polymers in DI water is shown in Figure 3. The pristine, uncut polymer sample (0.003 MBA:AMPS ratio) has a UT strength of 19.1 ± 2.4 MPa and a UT strain of 0.188 ± 0.044 (Figure 3a). After being cut in half and healed in the presence of DI water, the rejoined sample has a UT strength of 12.9 ± 4.1 MPa and a UT strain of 0.028 ± 0.007, which corresponds to healing efficiencies of 67.5 ± 21.6 and 15.0 ± 3.6%, respectively (Figure 3a,b). When the MBA:AMPS ratio is doubled to 0.006,



https://doi.org/10.1021/acsapm.3c00805
ACS Appl. Polym. Mater. 2023, 5, 6143−6150

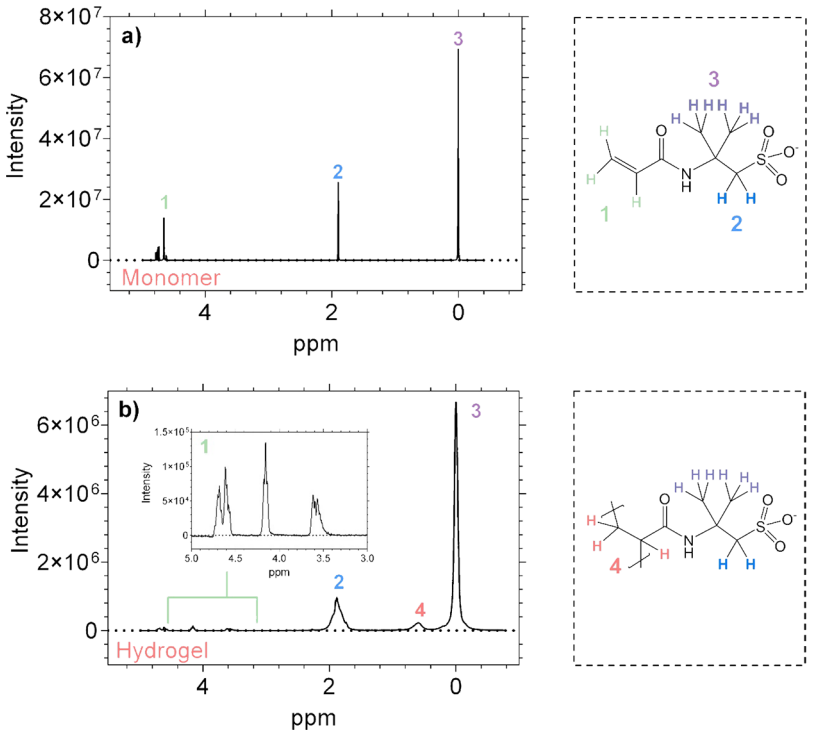


**Figure 2.** $^{1}$H NMR characterization. Hydrogel samples were obtained via a heat-initiated cationic polymerization of the monomer and crosslinker. $^{1}$H NMR spectroscopy was used to confirm the conversion of (a) 2-acrylamido-2-methyl-1-propane sulfonic acid to (b) poly(2-acrylamido-2-methyl-1-propane sulfonic acid). The conversion was verified by the decline in the intensity of the peaks that are associated with the hydrogen located around the double bond (labeled 1) and the appearance of the peak that corresponds to the new hydrogen environment created during polymerization (labeled 4).

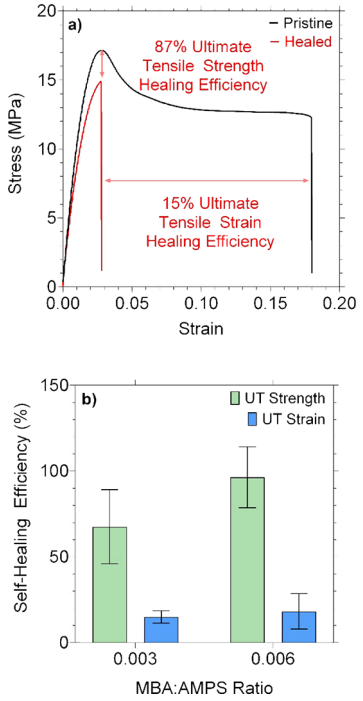


**Figure 3.** Quantifying self-healing efficiency via tensile stress−strain curves. Self-healing efficiency was measured by determining the percent recovery of bulk mechanical properties, specifically UT strength and strain. (a) The tensile stress−strain curves represent a pristine and healed hydrogel with 0.003 MBA:AMPS. Healing occurred in the absence of ions. (b) Self-healing efficiency for the 0.003 and 0.006 MBA:AMPS ratio showed similar efficiencies.

the UT strength of the pristine sample is 17.0 ± 2.18 MPa and the UT strain is 0.206 ± 0.058. At this higher crosslinker content, the samples recovered 96.3 ± 17.8% of their UT strength and 18.2 ± 10.3% of their UT strain (Figure 3b). At these MBA:AMPS ratios, the hydrogels display similar mechanical and self-healing properties. This was unexpected since it has been shown that higher crosslinker-to-monomer ratios improve the strength of a material and increase its rigidity.[36] In addition, higher crosslinker-to-monomer ratios typically reduce chain mobility, which can lower self-healing ability. However, certain ranges of crosslinker-to-monomer ratios may display similar healing efficiency. For example, a polyampholyte hydrogel with 0.01 and 0.02 crosslinker-to-monomer ratios exhibited healing efficiencies (based on strength at break) of 22.13 ± 8.82 and 19.17 ± 10.27%, respectively.[35] Our results indicate that the crosslinker-to-monomer ratios used for this study may fall within a range where bulk mechanical properties and mechanical property recovery for pristine samples and those healed with DI water are similar.

In some cases, the standard deviation for self-healing efficiencies is quite large, up to 34.5%. This could be attributed to the hydrogels being heterogeneous in structure.[37] The amount of the crosslinker present at and near the cut interfaces may vary, which would impact the mechanical properties of the material. Large standard deviation could also be attributed to how well the cut interfaces are realigned. Good realignment of interfaces is vital in facilitating self-healing because it allows for the reformation of bonds and interchain diffusion across the interfaces. If the alignment is poor, it will result in a lower self-healing efficiency (Figure S3). Even though good alignment for all samples was visually observed, there could be differences in


https://doi.org/10.1021/acsapm.3c00805
ACS Appl. Polym. Mater. 2023, 5, 6143−6150

surface roughness between the cut interfaces such that it impacts self-healing efficiency.

**3.3. Self-Healing of PAMPS Polymers in the Presence of Monovalent Ions.** The self-healing property of the 0.0030 MBA:AMPS polymers exposed to NaCl solutions is shown in Figure 4. The healed samples have UT strength healing efficiencies of 48.1 ± 1.85 and 44.1 ± 10.4% at NaCl concentrations of 17.25 and 35 g/L, respectively. The UT strain healing efficiencies were 31.0 ± 4.34 and 43.9 ± 16.9% at NaCl concentrations of 17.25 and 35 g/L, respectively. It was anticipated that the UT strength self-healing efficiency would be impaired by the presence of monovalent ions due to positively charged $Na^+$ ions disrupting hydrogen bonding.[25,26] The $Na^+$ ion would interact with the partially negative oxygen on the amide group or the fully negative oxygen on the sulfonic group. Figure 4a shows that these ions appear to hinder self-healing ability with respect to UT strength. The UT strength self-healing efficiency is lowered by ∼30% when we go from 0 g/L NaCl to 17.25 and 35 g/L NaCl (Figure 4a). Despite the concentration of NaCl being almost doubled, the self-healing efficiency based on UT strength is similar. This suggests that after reaching a certain ion concentration, the impact of NaCl on UT strength self-healing efficiency may plateau.

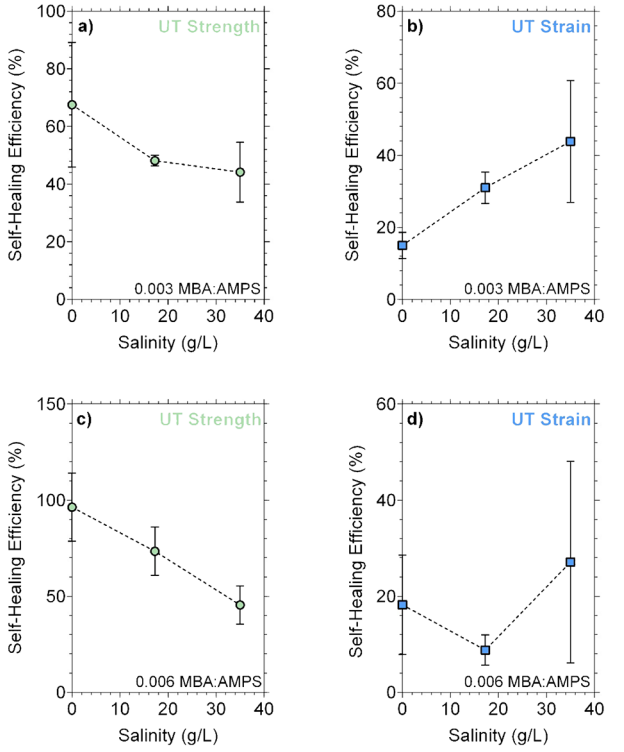


**Figure 4.** Self-healing efficiency at different sodium chloride (monovalent ion) concentrations. Self-healing efficiency was measured for 0.003 MBA:AMPS hydrogels (a, b) and 0.006 MBA:AMPS hydrogels (c, d). These MBA:AMPS ratios exhibit similar trends with increasing ion concentration hindering UT strength healing efficiency but improving or having little impact on UT strain healing efficiency. Note: The dashed line connecting the points is only present to guide the eye, and the error bars represent the standard deviation.

In contrast, it was expected that the UT strain self-healing efficiency would be improved in the presence of monovalent ions. Due to the positively charged $Na^+$ ions interfering with hydrogen bonding, the polymer chains would be able to slip by one another without "getting caught", i.e., forming hydrogen bonds, as they diffuse across the cut interface. Insight into polymer chain diffusion can be gained by comparing UT strain.[25] Figure 4b shows that as the NaCl concentration increases from 0 to 17.25 and 35 g/L, the UT strain self-healing efficiency improves by ∼15%. The self-healing efficiency based on UT strain is similar at 17.25 and 35 g/L, which was expected since the UT strength self-healing efficiencies were also similar at these concentrations. Generally, as the strength increases, the strain is hindered, and as the strength decreases, the strain is improved.

The self-healing property of the 0.006 MBA:AMPS polymers exposed to NaCl solutions is shown in Figure 4. The healed samples have UT strength healing efficiencies of 73.4 ± 12.6 and 45.4 ± 9.88% at NaCl concentrations of 17.25 and 35 g/L, respectively. The UT strain healing efficiencies were 8.79 ± 3.11 and 27.1 ± 21.0% at NaCl concentrations of 17.25 and 35 g/L, respectively. At this MBA:AMPS ratio, the UT strength self-healing efficiency followed a downward trend similar to what was seen for the 0.003 MBA:AMPS ratio UT strength self-healing efficiency (Figure 4c). In contrast, the UT strain self-healing efficiency appears to decrease at 17.25 g/L and then increase at 35 g/L (Figure 4d). However, given the fairly large standard deviation in the first and third data points, the UT strain self-healing efficiency values lie within the same range, and we cannot conclude that there is a specific trend.

**3.4. Self-Healing of PAMPS Polymers in the Presence of Divalent Ions.** The self-healing property of the 0.003 MBA:AMPS polymers exposed to $MgSO_4$ solutions is shown in Figure 5. The healed samples have UT strength healing efficiencies of 66.5 ± 3.23 and 35.0 ± 13.2% at $MgSO_4$ concentrations of 17.25 and 35 g/L, respectively. The healing efficiencies based on UT strain were 34.9 ± 9.25 and 111.8 ± 34.5% at 17.25 and 35 g/L $MgSO_4$, respectively.

Based on previous studies,[23,24,27] we hypothesized that the divalent ion $Mg^{2+}$ would form ionic bonds or metal−ligand coordination interactions with the fully negative oxygen on the sulfonic group. Due to this interaction, it was expected that the polymer samples would display a UT strength higher than those healed with DI water, while the UT strain would be lower than samples healed with DI water. However, samples healed in the presence of 35 g/L $MgSO_4$ displayed a UT strength healing efficiency that was ∼30% lower than the efficiency displayed for samples healed in the absence of ions (Figure 5a). This suggests that the $Mg^{2+}$ ions are behaving like the $Na^+$ ions and disrupting hydrogen bonding. Interestingly, at 17.25 g/L $MgSO_4$, the UT strength healing efficiency (66.5 ± 3.23%) is similar to the healing ability exhibited at 0 g/L $MgSO_4$ (67.5 ± 21.6%). A similar effect was seen for UT strain (Figure 5b). At 0 and 17.25 g/L $MgSO_4$, the UT strain healing efficiencies were 15.0 ± 3.6 and 34.9 ± 9.25%, respectively. However, at 35 g/L, the UT strain healing efficiency improved by ∼100% compared to samples healed with DI water. This large improvement in strain suggests that the $Mg^{2+}$ ions may be enhancing polymer chain diffusion more than the $Na^+$ ions (∼15% improvement). When $Mg^{2+}$ is hydrated, it has a radius of 0.428 nm, while hydrated $Na^+$ has a radius of 0.358 nm.[38] Due to $Mg^{2+}$ having a larger hydrated radius, it may cause the hydrogen bonding groups to be farther away from one another compared to when $Na^+$ is present. This could result in better interchain diffusion since the $Mg^{2+}$ ions may weaken the hydrogen bonding more than the $Na^+$. Therefore, the polymer chains may be able to diffuse more easily across the cut


https://doi.org/10.1021/acsapm.3c00805
ACS Appl. Polym. Mater. 2023, 5, 6143−6150

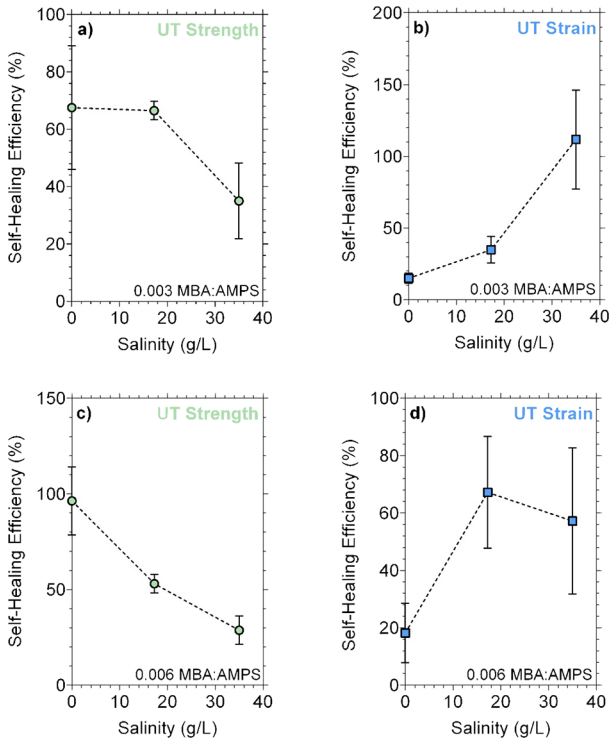


**Figure 5.** Self-healing efficiency at different magnesium sulfate (divalent ion) concentrations. Self-healing efficiency was measured for 0.003 MBA:AMPS hydrogels (a, b) and 0.006 MBA:AMPS hydrogels (c, d). These MBA:AMPS ratios exhibit similar trends with increasing ion concentration impairing UT strength healing efficiency but enhancing UT strain healing efficiency. Note: The dashed line connecting the points is only present to guide the eye, and the error bars represent the standard deviation.

interface in the presence of $Mg^{2+}$ than $Na^{+}$; i.e., the chains would be able to slip by one another without getting "caught" (forming hydrogen bonds). Greater interchain diffusion can lead to a higher strain.[25]

These findings imply that the $Mg^{2+}$ ion may not be acting as a crosslinker between partially or fully charged oxygen groups present on the polymer chain. $Mg^{2+}$ may have a higher affinity to interact with the surrounding water molecules.[39,40] In addition, the oxygen groups may not be oriented in a conformation favorable for $Mg^{2+}$ interactions.[41] These results also indicate that the system may have different regimes where multiple concentrations of $MgSO_4$ produce similar healing properties and that the concentration of $MgSO_4$ needs to reach a certain threshold before having an impact on healing. Another possibility could be that $Mg^{2+}$ ions are disrupting hydrogen bonding and forming ionic bonds or metal−ligand coordination interactions, but the disruption of hydrogen bonds is greater than the crosslink-like bonds being formed.

The self-healing property of a 0.006 MBA:AMPS polymer can be seen in Figure 5. The healed samples have UT strength healing efficiencies of 53.0 ± 4.93 and 28.7 ± 7.48% at $MgSO_4$ concentrations of 17.25 and 35 g/L, respectively. The UT strain healing efficiencies were 67.2 ± 19.5 and 57.2 ± 25.4% at $MgSO_4$ concentrations of 17.25 and 35 g/L, respectively. At this MBA:AMPS ratio, the UT strength self-healing efficiency followed a downward trend (Figure 5c) similar to what was seen for the 0.003 MBA:AMPS ratio UT strength self-healing efficiency. In contrast, the UT strain self-healing efficiency increased ∼40% in the presence of $MgSO_4$ (Figure 5d).

**3.5. Impact of the Crosslinker-to-Monomer Ratio on Self-Healing Efficiency.** The healing ability of two different crosslinker-to-monomer ratios, 0.003 and 0.006 MBA:AMPS, was studied to determine if and how the crosslinker influences self-healing in NaCl and $MgSO_4$ ion conditions. When comparing 0.003 and 0.006 MBA:AMPS hydrogels, we see that they display similar self-healing efficiencies and trends (Figure 6). This indicates that there may be ranges of crosslinker-to-monomer ratios where similar healing ability is exhibited, which could be useful to note when designing self-healing polymers for applications in complex matrices.

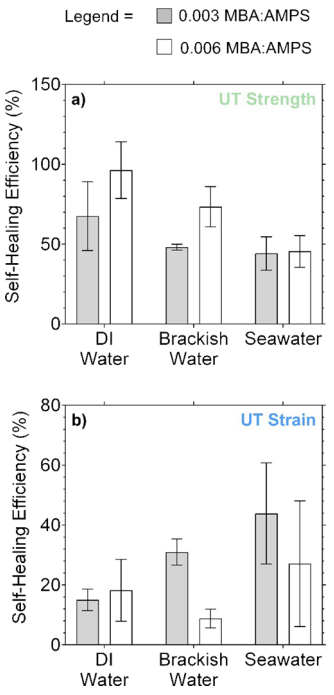


**Figure 6.** Impact of the crosslinker-to-monomer ratio on self-healing efficiency in sodium chloride conditions. Self-healing efficiency was calculated based on UT (a) strength and (b) strain. The error bars in these plots represent the standard deviation, and the data is the same as that seen in Figures 4 and 5 but has been replotted.

## 4. CONCLUSIONS

This work shows that certain divalent ions may not enhance self-healing ability by forming ionic or metal−ligand interactions. Under divalent ($MgSO_4$) as well as monovalent (NaCl) ion conditions, the UT strength self-healing efficiency declines as the salinity increases. In contrast, the UT strain self-healing efficiency improves with increasing ion concentration. From these findings, it may imply that self-healing polymers that primarily rely on hydrogen bonding for healing ability may not be ideal for underwater (brackish or seawater) applications that require high strength. Mechanistically, our findings suggest that $MgSO_4$ and NaCl ions may be disrupting hydrogen bonding and improving interchain diffusion. However, the mechanisms by which the ions are interacting with the hydrogen bonding groups cannot be confirmed through bulk mechanical testing.

To build upon the work completed in this study and continue advancing the field of self-healing polymers, further work should be conducted. This work should include gaining a better understanding of how these ions interact with polymer


https://doi.org/10.1021/acsapm.3c00805
ACS Appl. Polym. Mater. 2023, 5, 6143−6150

functional groups on a molecular level. In addition to elucidating the molecular interactions of NaCl and $MgSO_4$ ions with hydrogen bonding groups, the impact of other ions and common water constituents on self-healing should be explored. By studying how other ions influence healing ability, it can be determined if our conclusions can be generalized. Even though $Mg^{2+}$ does not appear to form ionic or metal−ligand bonds with the oxygen groups present, other ions may interact differently with such functional groups. For example, $Ca^{2+}$ strongly complexes with the oxygen groups present on polysaccharides such as alginate.[42,43] In addition, ions with the same charge can have different binding energies to the same functional group.[44] Further studies should also include examining self-healing properties in the presence of monovalent and divalent ions for hydrogen bonding-based systems without a negatively charged group. The absence of a negatively charged group could result in a larger disruption of hydrogen bonding due to ions solely interacting with the hydrogen bonding groups, i.e., no ionic interactions with a fully dissociated group. It may also be beneficial to study self-healing properties at different monomer weight percents as these polymers may be used at lower weight percents when incorporated into existing materials.[27,30] Through this type of work, the selection and design of self-healing materials for underwater, real-world applications can be improved.

## ■ ASSOCIATED CONTENT

### Supporting Information

The Supporting Information is available free of charge at https://pubs.acs.org/doi/10.1021/acsapm.3c00805.

FTIR analysis of monomer conversion to poly(2-acrylamido-1-propanesulfonic acid); FTIR spectra (Figure S1); number of parallel samples for different test conditions and MBA:AMPS ratios (Tables S1 and S2); optimizing hydrogel crosslinker-to-monomer ratio; parameters tested during crosslinker-to-monomer optimization (Table S3); swelling tests; swelling ratio calculation (eq S1); swelling ratio and ultimate tensile strength (Figure S2); alignment of samples during healing (Figure S3); impact of the crosslinker-to-monomer ratio on self-healing efficiency in magnesium sulfate conditions (Figure S4) (PDF)

## ■ AUTHOR INFORMATION


### Corresponding Author

**Bezawit A. Getachew** − *Department of Civil and Environmental Engineering, Rice University, Houston, Texas 77005, United States;* orcid.org/0000-0002-6757-5947; Email: bezawit.getachew@rice.edu

### Authors

**Durnian C. Parulski-Seager** − *Department of Civil and Environmental Engineering, Rice University, Houston, Texas 77005, United States;* orcid.org/0009-0005-4690-4368

**Amanda Suarez** − *Department of Civil and Environmental Engineering, Rice University, Houston, Texas 77005, United States*

Complete contact information is available at: https://pubs.acs.org/10.1021/acsapm.3c00805


### Notes

The authors declare no competing financial interest.

## ■ ACKNOWLEDGMENTS

The authors would like to thank the National Science Foundation for funding this work (Grant Number: 220136).

## ■ REFERENCES


(1) Wang, S.; Urban, M. W. Self-Healing Polymers. *Nat. Rev. Mater.* **2020**, *5*, 562−583.

(2) Guimard, N. K.; Oehlenschlaeger, K. K.; Zhou, J.; Hilf, S.; Schmidt, F. G.; Barner-Kowollik, C. Current Trends in the Field of Self-Healing Materials. *Macromol. Chem. Phys.* **2012**, *213*, 131−143.

(3) Taylor, D. L.; in het Panhuis, M. Self-Healing Hydrogels. *Adv. Mater.* **2016**, *28*, 9060−9093.

(4) Getachew, B. A.; Kim, S. R.; Kim, J. H. Self-Healing Hydrogel Pore-Filled Water Filtration Membranes. *Environ. Sci. Technol.* **2017**, *51*, 905−913.

(5) Kang, J.; Son, D.; Wang, G. J. N.; Liu, Y.; Lopez, J.; Kim, Y.; Oh, J. Y.; Katsumata, T.; Mun, J.; Lee, Y.; Jin, L.; Tok, J. B. H.; Bao, Z. Tough and Water-Insensitive Self-Healing Elastomer for Robust Electronic Skin. *Adv. Mater.* **2018**, *30*, 1706846.

(6) Zhang, F.; Ju, P.; Pan, M.; Zhang, D.; Huang, Y.; Li, G.; Li, X. Self-Healing Mechanisms in Smart Protective Coatings: A Review. *Corros. Sci.* **2018**, *144*, 74−88.

(7) Han, L.; Yan, L.; Wang, K.; Fang, L.; Zhang, H.; Tang, Y.; Ding, Y.; Weng, L. T.; Xu, J.; Weng, J.; Liu, Y.; Ren, F.; Lu, X. Tough, Self-Healable and Tissue-Adhesive Hydrogel with Tunable Multifunctionality. *NPG Asia Mater.* **2017**, *9*, e372−e372.

(8) Yang, Y.; Urban, M. W. Self-Healing of Polymers via Supramolecular Chemistry. *Adv. Mater. Interfaces* **2018**, *5*, 1800384.

(9) Billiet, S.; Hillewaere, X. K. D.; Teixeira, R. F.; Du Prez, F. E. Chemistry of Crosslinking Processes for Self-Healing Polymers. *Macromol. Rapid Commun.* **2013**, *34*, 290−309.

(10) Urban, M. W.; Davydovich, D.; Yang, Y.; Demir, T.; Zhang, Y.; Casabianca, L. Key-and-Lock Commodity Self-Healing Copolymers. *Sci.* **2018**, *362*, 220−225.

(11) Gong, J. P. Why Are Double Network Hydrogels so Tough? *Soft Matter* **2010**, *6*, 2583.

(12) Chen, Y.; Kushner, A. M.; Williams, G. A.; Guan, Z. Multiphase Design of Autonomic Self-Healing Thermoplastic Elastomers. *Nat. Chem.* **2012**, *4*, 467−472.

(13) Chen, Y.; Guan, Z. Multivalent Hydrogen Bonding Block Copolymers Self-Assemble into Strong and Tough Self-Healing Materials. *Chem. Commun.* **2014**, *50*, 10868−10870.

(14) Lai, J. C.; Jia, X. Y.; Wang, D. P.; Deng, Y. B.; Zheng, P.; Li, C. H.; Zuo, J. L.; Bao, Z. Thermodynamically Stable Whilst Kinetically Labile Coordination Bonds Lead to Strong and Tough Self-Healing Polymers. *Nat. Commun.* **2019**, *10*, 1164.

(15) Liu, J.; Tan, C. S. Y.; Yu, Z.; Li, N.; Abell, C.; Scherman, O. A. Tough Supramolecular Polymer Networks with Extreme Stretchability and Fast Room-Temperature Self-Healing. *Adv. Mater.* **2017**, *29*, 1605325.

(16) Sun, T. L.; Kurokawa, T.; Kuroda, S.; Ihsan, A. B.; Akasak, T.; Sato, K.; Haque, M. A.; Nakajima, T.; Gong, J. P. Physical Hydrogels Composed of Polyampholytes Demonstrate High Toughness and Viscoelasticity. *Nat. Mater.* **2013**, *12*, 932−937.

(17) Kessler, M. R.; Sottos, N. R.; White, S. R. Self-Healing Structural Composite Materials. *Composites, Part A* **2003**, *34*, 743−753.

(18) Bergman, S. D.; Wudl, F. Mendable Polymers. *J. Mater. Chem.* **2008**, *18*, 41−62.

(19) Syrett, J. A.; Becer, C. R.; Haddleton, D. M. Self-Healing and Self-Mendable Polymers. *Polym. Chem.* **2010**, *1*, 978.

(20) Murphy, E. B.; Wudl, F. The World of Smart Healable Materials. *Prog. Polym. Sci.* **2010**, *35*, 223−251.

(21) Yang, Y.; Urban, M. W. Self-Healing Polymeric Materials. *Chem. Soc. Rev.* **2013**, *42*, 7446−7467.

(22) Ekeocha, J.; Ellingford, C.; Pan, M.; Wemyss, A. M.; Bowen, C.; Wan, C. Challenges and Opportunities of Self-Healing Polymers and

Devices for Extreme and Hostile Environments. *Adv. Mater.* **2021**, *33*, 2008052.
(23) Xu, S.; Sheng, D.; Liu, X.; Ji, F.; Zhou, Y.; Dong, L.; Wu, H.; Yang, Y. A Seawater-Assisted Self-Healing Metal−Catechol Polyurethane with Tunable Mechanical Properties. *Polym. Int.* **2019**, *68*, 1084−1090.
(24) Li, J.; Ejima, H.; Yoshie, N. Seawater-Assisted Self-Healing of Catechol Polymers via Hydrogen Bonding and Coordination Interactions. *ACS Appl. Mater. Interfaces* **2016**, *8*, 19047−19053.
(25) Reisch, A.; Roger, E.; Phoeung, T.; Antheaume, C.; Orthlieb, C.; Boulmedais, F.; Lavalle, P.; Schlenoff, J. B.; Frisch, B.; Schaaf, P. On the Benefits of Rubbing Salt in the Cut: Self-Healing of Saloplastic PAA/PAH Compact Polyelectrolyte Complexes. *Adv. Mater.* **2014**, *26*, 2547−2551.
(26) Luo, F.; Sun, T. L.; Nakajima, T.; Kurokawa, T.; Zhao, Y.; Sato, K.; Ihsan, A. B.; Li, X.; Guo, H.; Gong, J. P. Oppositely Charged Polyelectrolytes Form Tough, Self-Healing, and Rebuildable Hydrogels. *Adv. Mater.* **2015**, *27*, 2722−2727.
(27) Getachew, B. A.; Kim, S. R.; Kim, J. H. Improved Stability of Self-Healing Hydrogel Pore-Filled Membranes with Ionic Cross-Links. *J. Membr. Sci.* **2018**, *553*, 1−9.
(28) Getachew, B. A.; Guo, W.; Zhong, M.; Kim, J.-H. Asymmetric Hydrogel-Composite Membranes with Improved Water Permeability and Self-Healing Property. *J. Membr. Sci.* **2019**, *578*, 196−202.
(29) Xing, X.; Li, L.; Wang, T.; Ding, Y.; Liu, G.; Zhang, G. A Self-Healing Polymeric Material: From Gel to Plastic. *J. Mater. Chem. A* **2014**, *2*, 11049−11053.
(30) Li, H. Q.; Liu, X. J.; Wang, H.; Yang, H.; Wang, Z.; He, J. Proton Exchange Membranes with Cross-Linked Interpenetrating Network of Sulfonated Polyvinyl Alcohol and Poly (2-Acrylamido-2-Methyl-1-Propanesulfonic Acid): Excellent Relative Selectivity. *J. Membr. Sci.* **2020**, *595*, No. 117511.
(31) Bakr, A. S. A.; Al-Shafey, H. I.; Arafa, E. I.; El Naggar, A. M. A. Synthesis and Characterization of Polymerized Acrylamide Coupled with Acrylamido-2-Methyl-1-Propane Sulfonic Acid-Montmorillonite Structure as a Novel Nanocomposite for Cd (II) Removal from Aqueous Solutions. *J. Chem. Eng. Data* **2020**, *65*, 4079−4091.
(32) Phetphaisit, C. W.; Yuanyang, S.; Chaiyasith, W. C. Polyacrylamido-2-Methyl-1-Propane Sulfonic Acid-Grafted-Natural Rubber as Bio-Adsorbent for Heavy Metal Removal from Aqueous Standard Solution and Industrial Wastewater. *J. Hazard. Mater.* **2016**, *301*, 163−171.
(33) Xiong, C.; Wei, F.; Ye, Z.; Feng, W.; Zhou, Q.; He, J.; Yang, H. An Injectable Self-Healing Hydrogel Based on Poly (Acrylamide-Co-N-Vinylimidazole) and Laponite Clay Nanosheets. *J. Appl. Polym. Sci.* **2023**, *140*, No. e53491.
(34) Cao, Y.; Wu, H.; Allec, S. I.; Wong, B. M.; Nguyen, D. S.; Wang, C. A Highly Stretchy, Transparent Elastomer with the Capability to Automatically Self-Heal Underwater. *Adv. Mater.* **2018**, *30*, 1804602.
(35) Ihsan, A. B.; Sun, T. L.; Kurokawa, T.; Karobi, S. N.; Nakajima, T.; Nonoyama, T.; Roy, C. K.; Luo, F.; Gong, J. P. Self-Healing Behaviors of Tough Polyampholyte Hydrogels. *Macromolecules* **2016**, *49*, 4245−4252.
(36) Anseth, K. S.; Bowman, C. N.; Brannon-Peppas, L. Mechanical Properties of Hydrogels and Their Experimental Determination. *Biomaterials* **1996**, *17*, 1647−1657.
(37) Di Lorenzo, F.; Seiffert, S. Nanostructural Heterogeneity in Polymer Networks and Gels. *Polym. Chem.* **2015**, *6*, 5515−5528.
(38) Nightingale, E. R., Jr. Phenomenological Theory of Ion Solvation. Effective Radii of Hydrated Ions. *J. Phys. Chem.* **1959**, *63*, 1381−1387.
(39) Bock, C. W.; Kaufman, A.; Glusker, J. P. Coordination of Water to Magnesium Cations. *Inorg. Chem.* **1994**, *33*, 419−427.
(40) Dudev, T.; Cowan, J. A.; Lim, C. Competitive Binding in Magnesium Coordination Chemistry: Water versus Ligands of Biological Interest. *J. Am. Chem. Soc.* **1999**, *121*, 7665−7673.
(41) Davis, T. A.; Llanes, F.; Volesky, B.; Mucci, A. Metal Selectivity of Sargassum Spp. and Their Alginates in Relation to Their α-L-Guluronic Acid Content and Conformation. *Environ. Sci. Technol.* **2003**, *37*, 261−267.
(42) Braccini, I.; Pérez, S. Molecular Basis of Ca2+-Induced Gelation in Alginates and Pectins: The Egg-Box Model Revisited. *Biomacromolecules* **2001**, *2*, 1089−1096.
(43) de Kerchove, A. J.; Elimelech, M. Formation of Polysaccharide Gel Layers in the Presenceof Ca2+ and K+ Ions: Measurements and Mechanisms. *Biomacromolecules* **2007**, *8*, 113−121.
(44) DuChanois, R. M.; Heiranian, M.; Yang, J.; Porter, C. J.; Li, Q.; Zhang, X.; Verduzco, R.; Elimelech, M. Designing Polymeric Membranes with Coordination Chemistry for High-Precision Ion Separations. *Sci. Adv.* **2022**, *8*, 9436.


https://doi.org/10.1021/acsapm.3c00805
*ACS Appl. Polym. Mater.* 2023, 5, 6143−6150